Applied Physics Letters

PERSPECTIVE | AUGUST 13 2024

Self-frequency-modulated laser combs

Mithun Roy ; Tianyi Zeng; David Burghoff

Appl. Phys. Lett. 125, 070503 (2024)
https://doi.org/10.1063/5.0215583

AIP Publishing

Applied Physics Letters PERSPECTIVE pubs.aip.org/aip/apl

Self-frequency-modulated laser combs

Cite as: Appl. Phys. Lett. **125**, 070503 (2024); doi: 10.1063/5.0215583
Submitted: 24 April 2024 · Accepted: 5 July 2024 ·
Published Online: 13 August 2024

Mithun Roy,[1,a] Tianyi Zeng,[2] and David Burghoff[1]

AFFILIATIONS

[1]Chandra Department of Electrical and Computer Engineering, Cockrell School of Engineering, The University of Texas at Austin, Austin, Texas 78712, USA
[2]John A. Paulson School of Engineering and Applied Science, Harvard University, Cambridge, Massachusetts 02138, USA

[a)]Author to whom correspondence should be addressed: mithunroy177@utexas.edu

ABSTRACT

Optical frequency combs with equidistant frequency modes have revolutionized metrology and spectroscopy. The most widespread combs consist of periodic pulse trains generated by mode-locked lasers. However, it has recently been demonstrated that most semiconductor lasers based on Fabry–Pérot cavities, such as quantum well laser diodes, quantum cascade lasers, and quantum dot lasers, can enter an unconventional regime without traditional mode-locking mechanisms. The time-domain profile of these self-locked combs features a frequency-modulated (FM) wave with quasi-continuous-wave intensity and near-linear frequency chirp. The observation of the FM mode of operation in lasers with significantly different dynamics suggested that this mode is a fundamental operating state of semiconductor lasers, stemming from a deeper underlying mechanism. Thanks to recent theoretical and experimental advances, the origin of FM behavior has become clear. In this Perspective, we discuss the current status of FM combs in semiconductor lasers based on Fabry–Pérot cavities, focusing on their physical origin, modeling, characterization, bandwidth enhancement, and potential in future applications.

I. INTRODUCTION

Since their inception, optical frequency combs have found numerous applications in precision spectroscopy, frequency synthesis, optical ranging, metrology, and quantum sources.[1–9] They are composed of discrete, equidistant lines in the frequency domain, and the phases of these lines determine their shape in the time domain. Frequency combs were first demonstrated using mode-locked lasers, which produce a periodic train of light pulses characteristic of amplitude modulation.[10,11] However, more recently, another class of combs has emerged characterized by an output that resembles frequency modulation (FM). These combs are mostly based on semiconductor lasers and produce a quasi-continuous-wave (quasi-CW) intensity with a frequency chirp.[12–16] Thanks to their broadband, flat-top, and quasi-CW nature, FM combs have potential for applications, such as optical communication and dual-comb spectroscopy.[17]

Frequency modulation of lasers was first achieved using an intracavity phase modulator,[18] shortly after the first successful demonstration of a laser.[19] Since the output intensity was low, direct measurement of the temporal profile could not be performed, and sinusoidal frequency modulation was assumed.[20] When mid-infrared (mid-IR) quantum cascade laser (QCL) combs were initially demonstrated, it was found that their output was not pulsed but rather quasi-CW.[21] Comb operation was seemingly achieved without any external or passive modulation. Shortly thereafter, the demonstration of a technique known as shifted wave interference Fourier transform spectroscopy (SWIFTS),[22,23] which employs linear detection through measuring the interferometrically modulated RF beatnote, made the temporal measurement of low, quasi-CW-like intensity profiles convenient. Unexpectedly, many QCLs were found to produce not a sinusoidally modulated output, but a linearly chirped FM.[12] This linearly chirped behavior has been demonstrated in other laser systems as well, such as quantum dot lasers,[13] quantum well diode lasers,[15] and interband cascade lasers.[14]

The fact that the linearly chirped behavior was observed in multiple laser platforms with vastly different dynamics suggested that this was a general state of laser dynamics. These laser systems were mainly simulated using the Maxwell–Bloch equations, either numerically or analytically using modal expansion methods.[24–29] Although they could reproduce the FM characteristics of the combs, they were not able to explain the essential mechanism responsible for producing FM combs with such distinct behavior. These equations were often composed of multiple coupled equations with many parameters, which made analysis difficult. However, by employing mean-field techniques similar to the Lugiato–Lefever formalism,[30,31] the coupled Maxwell–Bloch equations were recently reduced to just one equation,[32] which resembles the nonlinear Schrödinger equation (NLSE) but includes a phase

potential. This mean-field theory revealed that FM operation with a linear chirp is a general phenomenon in any laser with a Fabry–Pérot (FP) cavity, and it results from the motion of the gain grating. Specifically, an effective quasi-$\chi^{(3)}$ nonlinearity results from a combination of gain saturation and nonunity facet reflectivity. This nonlinearity creates a self-phase modulation, which causes the system to be governed by an NLSE with a phase potential. The fundamental solution to this equation is a field with quasi-CW intensity and linearly chirped frequency.[32]

In this Perspective, we discuss the current status of FM combs in semiconductor lasers based on FP cavities. Section II provides a brief account of experimental observations of FM combs across various laser platforms. In Sec. III, we discuss the modeling of FM combs, focusing on the mean-field theory. Section IV discusses several strategies to broaden the bandwidths of FM combs, while Sec. V focuses on characterizing the temporal profile of these combs. Finally, we conclude with a brief discussion on future research directions.

II. FUNDAMENTALS OF FM COMB OPERATION

FM combs form naturally in many semiconductor laser systems. For example, it has long been known that quantum well lasers can spontaneously (i.e., without any active or passive elements) enter a mode-locked regime, where the output intensity is almost constant.[33–35] In these cases, detailed measurements of the phase were not performed. Nevertheless, they were likely FM in nature.

Recently, a picture has emerged in which laser-based combs can be broadly classified into one of the four categories illustrated in Fig. 1, determined by whether they are formed by amplitude or phase modulation and whether the modulation is active or passive. Amplitude modulation yields classical mode-locking, producing time-domain pulses with near-zero intermodal phase. Active mode-locking employs external loss modulation, while passive mode-locking uses a saturable absorber that gives rise to self-modulation. When combs are formed via phase modulation instead, FM combs form. The phase counterpart of active mode-locking is the Fourier domain mode-locked laser (FDML), demonstrated in 2006.[36] Frequency chirping in FDML is achieved by driving an optical bandpass filter synchronously with the optical round trip time. Self-FM combs, discovered the most recently, can be considered counterparts to passive mode-locking, as they form in the cavity due to a phase-driven phase nonlinearity.

The discovery of QCL combs has generated interest in the potential applications and research of FM, as they do not favor traditional mode-locking regimes. QCLs can operate in both the mid-IR and THz regions, deliver high power, and lase at high temperatures,[38,39] which makes them appealing for applications, such as spectroscopy and radiometry.[17,40,41] Spontaneous comb operation has been demonstrated for both mid-IR and THz QCLs, with most devices employing dispersion compensation mechanisms. These include the use of broadband heterogeneous gain media,[21] double-chirped mirrors,[22] and structures similar to Gires–Tournois etalons.[42] Mid-IR QCLs typically produce quasi-CW intensities with a linear frequency sweep [Fig. 2(c)], whereas

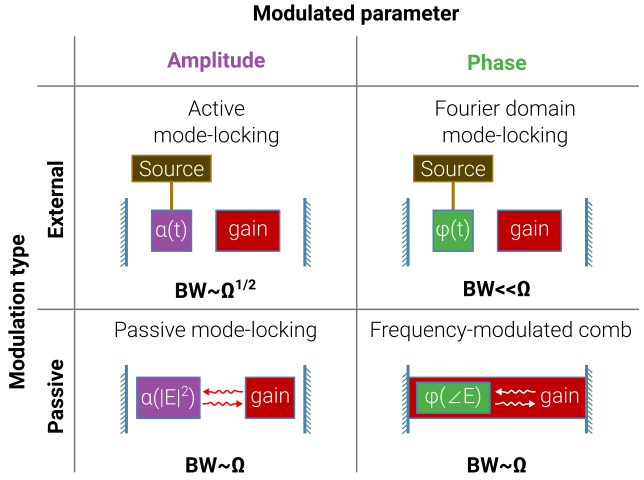

FIG. 1. Overall landscape of laser-based combs.[37] Traditional mode-locking produces amplitude-modulated output, while FDML and FM combs produce output with quasi-CW intensity. Ω represents the gain bandwidth (full-width-at-half-maximum). The output bandwidths for externally modulated lasers are smaller than those for their passive counterparts. Roy *et al.*, arXiv:2310.00028 (2024); licensed under a Creative Commons Attribution (CC BY) license.

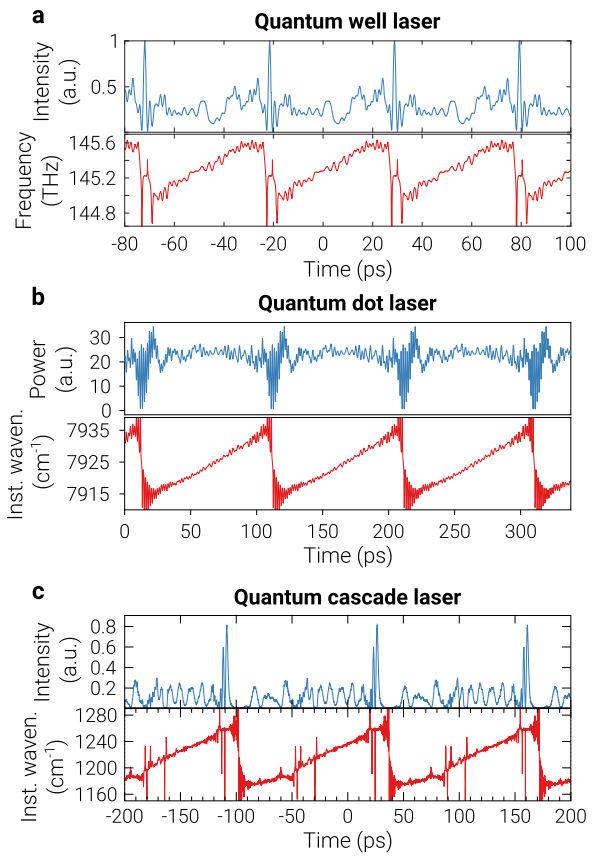

FIG. 2. SWIFTS characterization of temporal profiles of FM combs in a (a) quantum well laser,[15] (b) quantum dot laser,[13] and (c) mid-IR QCL.[12] Although the physical parameters for these lasers were different, they all locked spontaneously, producing combs with quasi-CW intensity and linear frequency chirp. Reproduced from Sterczewski *et al.*, APL Photonics **5**, 076111 (2020), with the permission of AIP Publishing. Hillbrand *et al.*, Phys. Rev. Lett. **124**, 023901 (2020); licensed under a Creative Commons Attribution (CC BY) license. Reproduced with permission from Singleton *et al.*, Optica **5**, 948 (2018). Copyright 2018 Optica Publishing Group.[12]

THz QCLs tend to produce pulse-like intensities with less distinct chirp,[43] attributed to their longer gain recovery times. Recently, by employing a tapered FP cavity, a linear frequency chirp has been demonstrated in THz QCLs.[44] Moreover, a novel FM state characterized by a broad, flat spectrum with a discontinuous cosine phase has been demonstrated in mid-IR ring QCLs very recently;[45] however, such states do not form spontaneously, requiring strong RF injection. Temporal characteristics of QCLs have been measured using a variety of recently developed techniques, including not only SWIFTS but also Fourier-transform analysis of comb emission (FACE)[43] and asynchronous upconversion sampling (ASUPS).[46,47]

While the earliest signatures of self-FM formation occurred in quantum well lasers, FM operation was only recently confirmed in them. In Ref. 15, a GaSb-based quantum well laser was reported to produce FM combs. The device was single-section and based on an FP cavity, and under less than 500 mW of electrical bias, the device produced a quasi-flat optical spectrum with ∼1.5 THz of bandwidth. The measurement of temporal intensity and intermodal phase was performed using SWIFTS, revealing a maximally chirped FM state with phases distributed linearly between $-\pi$ and π and a quasi-CW intensity (with pronounced spikes at points where the laser changes the direction of its frequency sweep). The reconstructed instantaneous intensity and frequency are shown in Fig. 2(a). FM operation with a linear frequency chirp was also demonstrated in InGaAsP-based laser diodes.[48]

Quantum dot lasers have also been shown to produce FM combs. Due to their immunity to growth defects, ultra-low threshold currents, high-temperature operation, and broad spectral coverage,[49–51] quantum dot lasers are very attractive for integrated frequency comb technologies. Hillbrand *et al.*[13] investigated a 4 mm long monolithic InAs/InGaAs quantum dot laser operating at around 1.27 μm. SWIFTS temporal measurements showed that the device, under uniform DC bias, produced an almost constant intensity profile [Fig. 2(b)] with intermodal phases splayed linearly across the full range of 2π. Similar FM-like behavior was reported in InAs/InGaAsP quantum dash lasers as well.[52] Interband cascade laser is another laser system known to operate in the FM comb regime. Using a two-section device, where the shorter section was used for dispersion compensation, Schwarz *et al.*[14] reported a spontaneous comb with a bandwidth of ∼1.15 THz and a linear frequency chirp.

III. THEORY OF FM COMBS

Like all lasers, FM combs can be modeled and investigated using the Maxwell–Bloch equations, which use Maxwell's equations to describe light propagation and the Bloch equations to describe the dynamics of a two or more level system. One can solve these equations by adopting two approaches. The first approach involves solving the population, coherence, and Maxwell's equations directly in the spatiotemporal domain,[24–27] although this is computationally intensive and offers less visualization due to all the equations being coupled. In the second approach, one can assume the facet reflectivities to be unity and express the modes in an FP cavity as having cosine forms, simplifying the analysis to require solving in the time domain only.[28,29] Although more intuitive, this method fails to naturally produce essential characteristics of an FM comb, such as a linear frequency chirp. In pursuit of a more rigorous yet simplified model, Opacak and Schwarz[53] proposed a spatiotemporal model in which the Maxwell–Bloch equations were reduced to only two equations for fast gain media enclosed in an FP cavity. This model could produce all the FM comb characteristics observed in experiments, including the linear chirp behavior. Shortly thereafter, using a mean-field formalism, Burghoff[32] simplified the Maxwell–Bloch equations to a single equation, albeit one involving convolutions. When some weak assumptions are applied, this simplifies to the simplest description of FM comb formation proposed to date. Unlike the conventional nonlinear Schrödinger equation, which is governed by an intensity potential, this equation is governed by a generalized version with a phase potential. Importantly, this is derived from first-principles and allows for analytical descriptions of FM combs to be formed. A related spatiotemporal equation has also been derived very recently based instead on an order parameter approach.[54]

A. Mean-field theory

The mean-field theory can be derived following a similar approach to that of the Lugiato–Lefever equation (LLE), which plays an instrumental role in understanding the formation of Kerr combs in microresonators.[31] Three main steps need to be followed to derive the final equation. The first step involves reducing the coupled Maxwell–Bloch equations into two equations—one for forward- and the other for backward-propagating waves—using the adiabatic approximation. These equations are typically referred to as the master equations.[32,53,55] In the second step, the backward-propagating wave is flipped and the FP cavity is extended, thus reducing the two equations into one equation containing a single forward-propagating wave. In the third step, one needs to integrate the resulting equation over a round trip. However, unlike microresonators, the challenge is that the intracavity gain in semiconductor lasers is large within a round trip and cannot be neglected. Moreover, the mirror losses cannot be neglected, as is commonly done.[30,31] In fact, mirror losses are essential to the operation of FM combs. This problem can be addressed by normalizing the electric field to a scaling function, which is found using the steady-state power profile of the laser (the power produced by a laser without any phase-dependent terms). Finally, by integrating the equation over a round trip, one gets the spatiotemporal mean-field equation as follows:

$$\frac{\partial F}{\partial T} = i\frac{1}{2}\beta\frac{\partial^2 F}{\partial z^2} + \frac{1}{4}D_g\frac{\partial^2 F}{\partial z^2} - \tilde{K}\left[\gamma_1\frac{\partial F^*}{\partial z}F + \gamma_2 F^*\frac{\partial F}{\partial z}\right]F - \frac{1}{3}r\left(|F|^2 + 2\langle K\rangle^{-1}\tilde{K}\left[|F|^2\right] - 3P_0\right)F, \quad (1)$$

where F is the normalized slow-intensity envelope, T denotes the slow time (usually expressed in fractional units of the round trip time), β represents the normalized group velocity dispersion, D_g represents gain curvature, P_0 is the steady-state power at the left cavity facet, K is a dimensionless power gain that the field experiences as it traverses the cavity, and the angle brackets denote an average over position. Moreover, r is the energy-relaxation parameter and is a function of the peak gain, saturation intensity, and $\langle K\rangle$. The notation $\tilde{K}[f](z)$ represents the convolution of $K(z)$ and an arbitrary function $f(z)$. The convolution arises because the cavity possesses both the forward- and backward-propagating waves. Furthermore, γ_1 and γ_2 represent the nonlinear cross-steepening and are functions of the population lifetime T_1 and coherence lifetime T_2. These cross-steepening terms arise due to temporal variation of the gain grating. The convolution involving K makes this formalism somewhat more complicated than the standard

LLE and FP-LLE formalisms. However, this equation can be readily solved using Fourier methods, such as the split-step method.

B. Phase NLSE and origin of phase modulation

If one makes certain simplifying assumptions, namely, assuming zero gain curvature and linear growth of the steady-state power, the mean-field equation simplifies to the following phase-driven NLSE:

$$-i\frac{\partial F}{\partial T} = \frac{\beta}{2}\frac{\partial^2 F}{\partial z^2} + \gamma|F|^2(\angle F - \langle \angle F\rangle)F + ir(|F|^2 - P_0)F. \quad (2)$$

Here, $\gamma = (\gamma_1 - \gamma_2)\Delta P/(4L_c P_0)$, ΔP is the power loss at the facet(s), and L_c is the cavity length. This equation looks more like the conventional NLSE with one significant difference: the conventional NLSE is governed by an intensity potential while the phase NLSE is dictated by a phase potential. The expression of γ reveals the two key ingredients to FM comb formation: (1) *large power discontinuity at the facets and* (2) *cross-steepening*. Note that in the absence of backward-propagating field, for instance, in a unidirectional ring QCL,[56,57] such cross-steepening interaction does not occur. In Fig. 3(a), the various steps to derive the phase NLSE from the Maxwell–Bloch equations are presented in the form of an inverted pyramid. Reference 32 shows that this differential equation has an analytical solution, which is a field characterized by a linear frequency chirp. In Fig. 3(b), both the numerical and analytical solutions to the phase NLSE are presented, showing their excellent agreement except at the point (boundary) where the instantaneous frequency is discontinuous. An amplitude pulsation appears at the boundary, which was observed in experiments as well (Fig. 2). Solutions of this nature were referred to as extendons to emphasize their spatially extended nature.

C. Interplay between gain curvature and comb stability

An important and relevant question is what the ultimate bandwidth limits are for FM combs. For pulsed lasers, the bandwidth limits are well-established and are provided by the Haus theory.[58,59] Specifically, for actively mode-locked lasers, the output bandwidth is proportional to the square root of the gain bandwidth (full-width-at-half-maximum) Ω (Fig. 1). Pulse widths can be further reduced in passively mode-locked lasers, where the bandwidth scales linearly with Ω. For chip-scale devices utilizing the FDML scheme, the achievable bandwidth is typically much narrower than Ω, due to the difficulty associated with broadly tuning a filter at the repetition rate. By contrast, the bandwidth limits for FM modes of operation were not fully understood, mainly due to the challenges of handling the multiple coupled Maxwell–Bloch equations. However, the development of the mean-field theory has paved the way for a simpler framework, making it possible to estimate the limits.

It is widely accepted that the bandwidth of a comb can be increased through dispersion compensation. However, the mean-field theory suggests that this is not the complete story, as gain curvature plays a crucial role in determining the bandwidth and stability of an FM comb. In the absence of gain curvature, the comb remains stable for any value of dispersion selected, and the bandwidth of the comb can be made arbitrarily large by reducing dispersion. When gain curvature is enabled, this is no longer true. By simulating the mean-field theory numerically, it has recently been shown that the minimum value of dispersion required to form a stable extendon depends on gain curvature.[37] This minimum value can also be referred to as the optimum dispersion. In particular, the optimum dispersion has been found to increase quadratically with gain curvature for a typical mid-IR and THz QCL. For values of dispersion smaller than the optimum dispersion, severe amplitude fluctuations would develop, resulting in the destabilization of the comb. Since the comb bandwidth and effective gain bandwidth are determined by the optimum dispersion and gain curvature, respectively, it has also been shown that the comb bandwidth is *proportional* to the system's effective gain bandwidth,[37] similar to the case of a passively mode-locked laser. This linear behavior has been found to

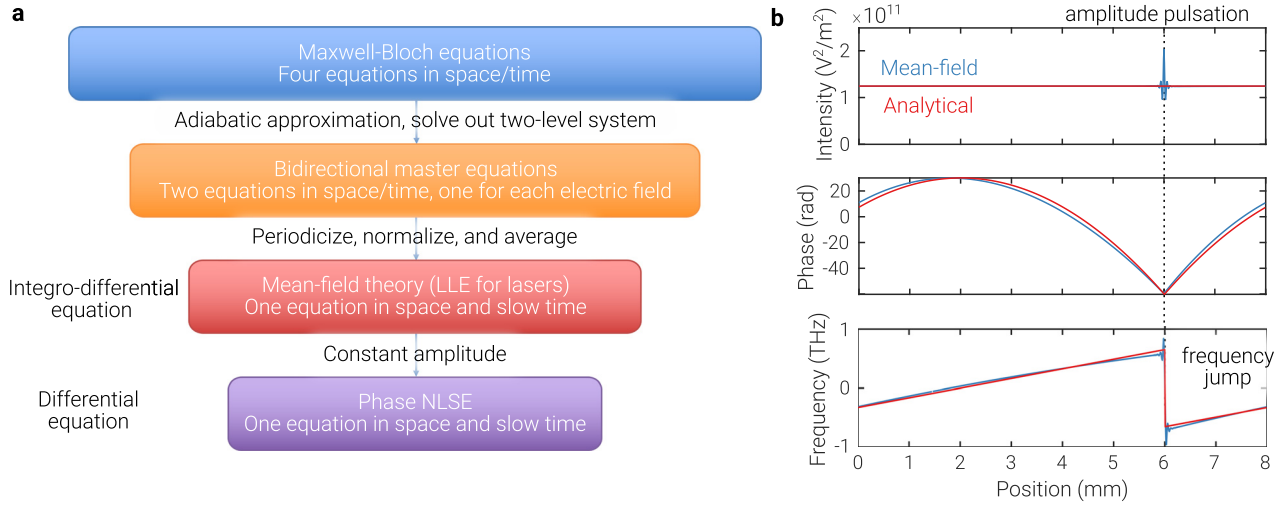

FIG. 3. Overview and relationship between various theoretical approaches. (a) General procedure that can be used to simplify the Maxwell–Bloch equations into phase NLSE. (b) Comparison between the numerical and analytical solutions to the phase NLSE, showing an excellent agreement except at the point where the instantaneous frequency is discontinuous. At this point, an intensity pulsation occurs.

hold across a broad parameter space for QCLs, suggesting its applicability to any FM comb based on fast gain media.

Kerr nonlinearity is not required to form FM combs. As long as the two essential ingredients, a gain grating and nonunity facet reflectivity, are present, any FP laser can in principle generate FM combs. However, the presence of Kerr nonlinearity will shift the range of dispersion for which a stable extendon can form.[32,53] It has been shown that Kerr nonlinearity, in conjunction with gain curvature, creates an effective dispersion of $\beta_{\text{eff}} = \beta - (1/2r)D_g\gamma'_K$, thus causing the shift. Here, γ'_K is the normalized Kerr nonlinearity coefficient.

IV. BROADENING COMB BANDWIDTH

Broad bandwidths are essential for most comb applications. In spectroscopy, broad bandwidth enables the detailed analysis of complex spectra, improving the identification and quantification of substances in chemical and biological research works.[60] In optical communications, a wider bandwidth means that more data can be transmitted over a single channel or fiber. This leads to increased data rates and capacity, meeting the growing demand for bandwidth due to high-definition video streaming, cloud computing, and other data-intensive applications. In this section, several strategies to enhance the bandwidth of FM combs are discussed.

Dispersion in a laser originates from the underlying material, waveguide, and the gain/loss in the active region. While a minimum amount of dispersion is necessary (the optimum dispersion) for comb stabilization, higher dispersion values are detrimental to comb formation. Using the mean-field theory, it can be shown that the bandwidth of an FM comb is inversely proportional to the dispersion.[32] Several strategies for dispersion compensation have been explored, as documented in various studies. For instance, Ref. 21 demonstrated a gain-medium-engineering approach, which involved growing three active regions with slightly differing center frequencies in a cascaded manner to create a heterogeneous mid-IR QCL. This design resulted in low group velocity dispersion due to the gain's flat-top profile [Fig. 4(a)]. For GaAs, the material commonly used in THz QCLs, material dispersion in the THz range significantly exceeds that in the mid-IR region, being over two orders of magnitude higher. Consequently, dispersion compensation becomes crucial for the operation of THz QCL combs. Reference 22 presented a method where chirped corrugations were etched onto the laser waveguide, effectively functioning as a double-chirped mirror [Fig. 4(b)]. These corrugations modulate the waveguide's width, altering the effective refractive index and introducing dispersion. With a precise design, this induced dispersion can be adjusted to balance the system's overall dispersion. Another electromagnetic scheme was adopted in Ref. 42 where a structure similar to a Gires–Tournois interferometer was integrated on the back facet of a mid-IR QCL [Fig. 4(c)]. The structure was composed of several layers of Al_2O_3 and SiO_2 and terminated with a gold layer. Like a double-chirped mirror, a Gires–Tournois etalon can also introduce dispersion, which can be controlled by varying the length and refractive index of the material.

Unlike mid-IR QCLs, THz QCLs based on an FP cavity do not readily produce a pure FM comb with a linear chirp. However, Ref. 44 recently reported FM comb operation with a linear chirp and flat spectra in THz QCLs by employing a tapered FP cavity [Fig. 4(d)]. At low temperatures (40 K), the devices generated combs with bandwidths comparable to those of non-tapered FP devices. However, at higher temperatures (97 K and above), the tapered devices produced broader bandwidth combs. This improvement was attributed to the increased field intensity from tapering, which boosts the efficiency of the gain saturation that leads to cross-steepening.

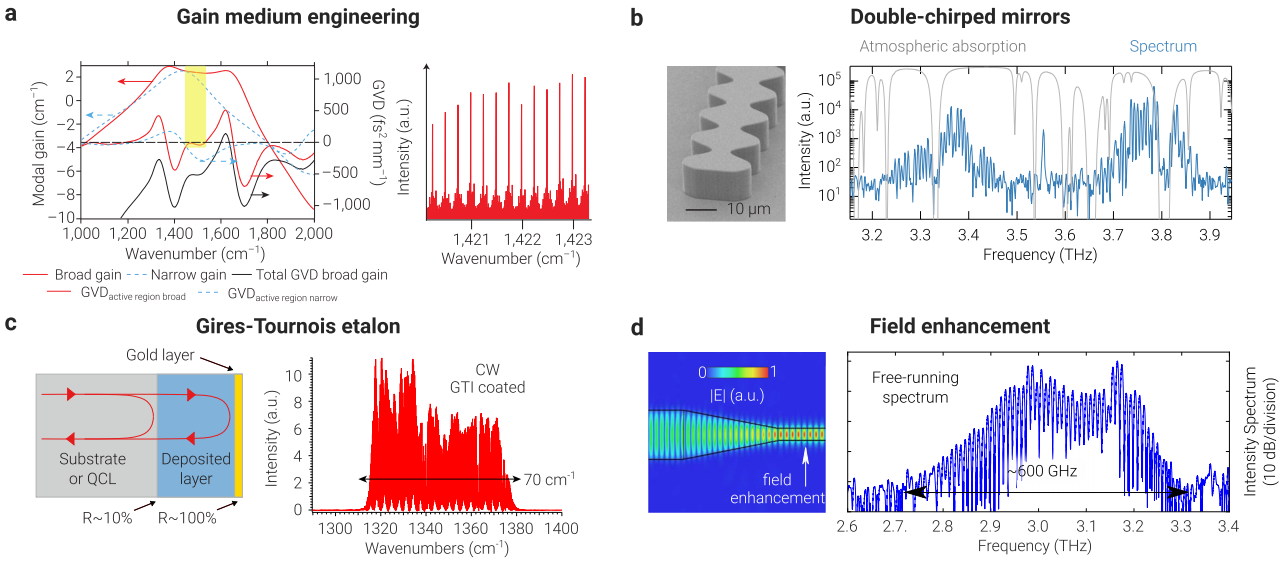

FIG. 4. Strategies for generating broader bandwidth combs. Dispersion compensation by (a) employing a heterogeneous QCL gain medium,[21] (b) etching chirped corrugations onto the THz QCL waveguide,[22] and (c) integrating a Gires–Tournois etalon on the facet of the QCL.[42] GTI, Gires–Tournois interferometer. (d) Enhancing field intensity by employing a tapered FP cavity.[44] At temperatures around 97 K and above, this strategy produced FM combs broader than that generated by a non-tapered FP QCL. Reproduced with permission from Hugi *et al.*, Nature **492**, 229–233 (2012). Copyright 2012 Springer Nature Limited. Reproduced with permission from Burghoff *et al.*, Nat. Photonics **8**, 462–467 (2014). Copyright 2014 Springer Nature Limited. Reproduced with permission from Villares *et al.*, Optica **3**, 252–258 (2016). Copyright 2016 Optical Society of America.[42] Senica *et al.*, Laser Photonics Rev. **17**, 2300472 (2023); licensed under a Creative Commons Attribution (CC BY) license.

Given that the optimum dispersion, which primarily determines comb bandwidths, increases with gain curvature, a strategy has been recently demonstrated that involves reducing gain curvature electromagnetically to broaden comb bandwidths.[37] The concept was demonstrated on THz QCL combs. Specifically, small disks were introduced on both sides of an FP laser cavity, spanning almost its entire length. Each of the disks was the QCL gain medium in a metal–metal waveguide. The disk parameters were carefully chosen to introduce resonant loss with the same center frequency as that of the gain, thus reducing the gain curvature of the net gain. The resonant loss was referred to as the anti-diffusive loss as its effect can be viewed as adding negative diffusion to Eq. (1).

V. CHARACTERIZING FM COMBS

The emission of a frequency comb differs from an incoherent multimode laser in that a definite phase relationship between the modes exists. Since FM combs are not pulses, conventional methods that rely on pulse-induced optical nonlinearities, such as FROG and interferometric autocorrelation, are unsuitable for examining their phases. In addition, determining the temporal profile of a comb is crucial, as it can reveal information about the physical mechanisms responsible for comb formation. This section focuses on several methods suitable for characterizing FM combs.

SWIFTS is a linear interferometric phase-sensitive technique, proposed concurrently with the initial demonstration of spontaneous comb operation in a THz QCL.[22] Given its ease of implementation, most laser-based FM combs have been characterized using SWIFTS. In this scheme, a fast optical detector is used to measure both the normal interferogram and beatnote as a function of the delay of an interferometer. The beatnote is then used as the source of an I/Q demodulator, and an in-phase signal $[S_I(\tau)]$ and an in-quadrature signal $[S_Q(\tau)]$ are detected using the repetition rate of the laser as a local oscillator [Fig. 5(a)]. These in-phase and in-quadrature signals can be used to define

$$X_{\pm}(\omega) = \frac{1}{2}\left(S_I(\omega) \mp iS_Q(\omega)\right), \tag{3}$$

which is often referred to as the SWIFTS correlation spectrum. Here, $S_I(\omega)$ and $S_Q(\omega)$ are the Fourier transforms of $S_I(\tau)$ and $S_Q(\tau)$, respectively. The correlation can also be written as $X_{\pm}(\omega) = \langle E^*(\omega)E(\omega \pm \Delta\omega)\rangle$, where $E(\omega)$ is the Fourier transform of the electric field and $\Delta\omega$ is the repetition rate, and the angle brackets represent an average over laboratory timescales. For incoherent light sources, the long-term phase incoherence between $E^*(\omega)$ and $E(\omega \pm \Delta\omega)$ will cause the integration to become zero. Therefore, the correlation is highly sensitive to the equidistance between the modes and can be used to prove comb coherence. Moreover, using the normal interferogram, one can define a spectrum product as $X_{sp\pm}(\omega) = \sqrt{\langle|E(\omega)|^2\rangle\langle|E(\omega\pm\Delta\omega)|^2\rangle}$. The degree of agreement between $X_{\pm}(\omega)$ and $X_{sp\pm}(\omega)$ serves as an additional measure of comb coherence [Fig. 5(b)]. Note that SWIFTS cannot verify the coherence between lines separated by a spectral gap that is larger than the detector's bandwidth.

One of the attractive features of SWIFTS is that it can be used to retrieve phase information, thereby determining the time-domain behavior of a comb. Since $\angle X_+(\omega) = \angle E(\omega + \Delta\omega) - \angle E(\omega)$, one can find the phases of a comb field, correct up to a global phase, by the cumulative summation of the SWIFTS phases. However, for an ultrabroadband comb, this phase retrieval process might not be robust since the noise associated with each line would cumulatively add, potentially overwhelming the measurement. Therefore, determining instantaneous frequency is preferable as it is not particularly sensitive to global phase and noise accumulation.

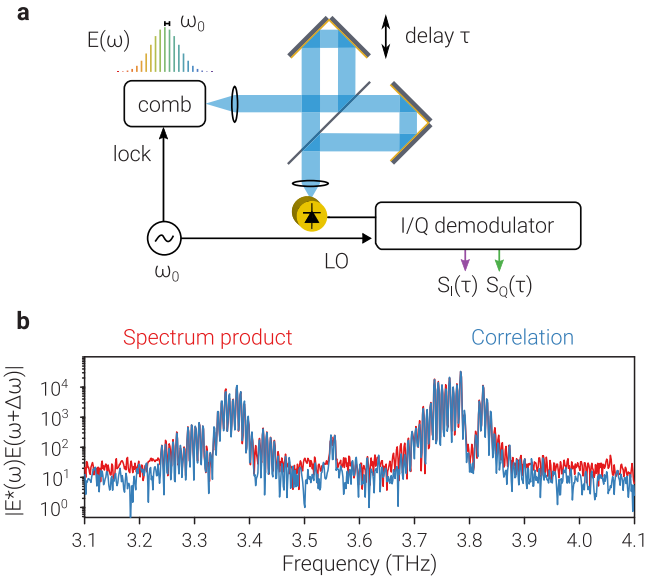

FIG. 5. (a) Experimental setup for SWIFTS.[23] (b) SWIFTS correlation spectrum and the spectrum product.[22] The latter was obtained using the normal interferogram, and their excellent agreement proved comb coherence. Reproduced with permission from Burghoff *et al.*, Opt. Express **23**, 1190 (2015). Copyright 2015 Optical Society of America.[23] Reproduced with permission from Burghoff *et al.*, Nature Photonics **8**, 462–467 (2014). Copyright 2014 Springer Nature Limited.

FACE[43] is a technique based on dual-comb detection. The sample comb (to be measured) is downconverted into the RF domain by beating it with a local oscillator comb (LO-FC) which acts as a reference comb [Fig. 6(a)]. The repetition rates for both combs need to be stabilized, and the offset frequency (and its noise) corresponding to the downconverted comb can be eliminated electronically. By measuring the downconverted comb signal as a time trace and performing Fourier transform analysis, the frequency, amplitude, and phase of the beatnotes can be retrieved. This ultimately allows for the reconstruction of the instantaneous intensity and frequency of the sample comb, since it has a one-to-one correspondence with the downconverted comb.

Unlike SWIFTS, which is a technique based on frequency domain measurements, ASUPS[46,47] is based on optical sampling in the time domain. Figure 6(b) shows the experimental configuration. The beam from a QCL passes through a tunable optical bandpass filter system, in which a movable slit performs the filtering. The QCL output is then spatially combined with the output from a femtosecond mode-locked laser, and the combined signal is guided through an $AgGaS_2$ crystal. The beams interact nonlinearly inside the crystal, and optical sampling is achieved through the frequency upconversion of the femtosecond pulses via sum-frequency generation. The sum-frequency signal is separated from the pump beams using a polarizing beam splitter and bandpass filters and measured on an avalanche photodiode. A phase

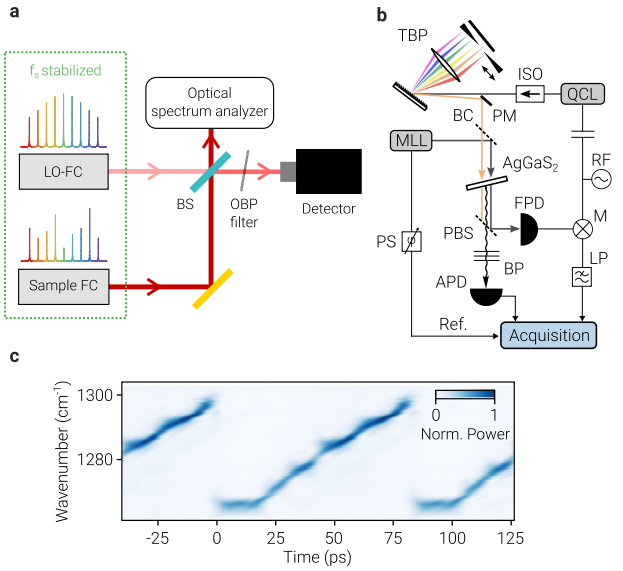

FIG. 6. Experimental configurations for (a) FACE[43] and (b) ASUPS.[47] BS, beam splitter; OBP, optical bandpass filter; TBP, tunable optical bandpass filter; ISO, optical isolator; PM, pickoff mirror; BC, beam combiner; RF, radio frequency synthesizer; FPD, fast (∼15 GHz) photodiode; M, frequency mixer; PS, phase shifter; PBS, polarizing beam splitter; LP, low pass filter; BP, optical bandpass filters; APD, avalanche photodiode. (c) Spectrogram for a mid-IR QCL measured using the tunable optical bandpass filter (ASUPS). The spectrogram displays a linear chirp in the wavenumber. Reproduced with permission from Cappelli *et al.*, Nat. Photonics **13**, 562–568 (2019). Copyright 2019, The Author(s), under exclusive license to Springer Nature Limited. Taschler *et al.*, Laser Photonics Rev. **17**, 2200590 (2023); licensed under a Creative Commons Attribution (CC BY) license.

shifter is used to sample the peak of each pulse impinging on the photodiode. Moreover, the frequency difference $\Delta f = |f_r\ (\mathrm{QCL}) - m f_r\ (\mathrm{fs\ laser})|$, where f_r is the repetition rate of the corresponding laser and m is the index of the femtosecond laser beatnote closest to f_r (QCL), is acquired by mixing the two frequency components electrically and filtering the product with a low-pass filter.

The instantaneous intensity profile is reconstructed by averaging the sum-frequency signal. Instantaneous frequency is obtained using the slit within the tunable bandpass filter system. The slit's width is adjusted to allow a portion of the QCL spectrum to pass through. Moving the slit stepwise across the entire QCL spectrum produces pulses with varying group delays. By measuring each pulse's center frequency using a Fourier transform spectrometer, a spectrogram similar to that in Fig. 6(c) can be generated. This spectrogram reveals the instantaneous frequency, where a well-defined pattern indicates comb coherence. One of the main advantages of ASUPS over autocorrelation techniques is the requirement of only a few milliwatts of comb power,[47] as opposed to the watt-level power required by the latter. Another related time-domain sampling technique was used in Ref. 61 to characterize an actively mode-locked THz QCL.

VI. CONCLUSION AND OUTLOOK

In the early years of frequency combs, most effort went into the development of mode-locked pulsed lasers, primarily due to their applications in optical metrology and atomic clocks. Now that the FM state of operation has been identified as the natural, favored state for most semiconductor lasers, FM combs have started gaining more prominence. Perhaps the most notable application of FM combs demonstrated to date is dual-comb spectroscopy.[17] In this scheme, two combs with known profiles and slightly different repetition rates are mixed,[62,63] similar to the FACE approach discussed in Sec. V. However, in this context, one of the combs is typically passed through a sample, and information about the sample's absorption characteristics is obtained by measuring the RF comb. Compared to methods based on Fourier-transform spectroscopy, this process is faster and does not require mechanically moving parts. Another potential application for FM combs is in dense wavelength-division multiplexing systems. Since FM combs are typically flat and broadband, with comb teeth having comparable power levels, all the comb lines can be utilized for data transmission—a crucial feature for the multiplexing systems.[64] Moreover, the efficiency of FM combs is extremely high and essentially identical to the efficiency of a continuous wave laser.

The repetition rates of most semiconductor FM combs demonstrated so far are in the gigahertz range, rendering them unsuitable for applications that require narrower frequency spacings. For instance, in gas spectroscopy of small molecules, the absorption linewidths are typically in the range of hundreds of megahertz at low pressures. Thus, moving forward, developing denser and tunable FM combs could be a key area of focus. Furthermore, unlike mid-IR and near-IR combs, which exhibit essentially pure FM behavior with a linear chirp, THz combs display signs of significant amplitude modulation, leading to less flat spectra. Improving the FM behavior of THz combs is another area that demands further research. Deepening the understanding of the physical mechanisms and their interplay is also crucial for fully unlocking the potential of FM combs in spectroscopy and beyond. FM combs could have a major impact even at shorter wavelengths. For example, despite the impressive development of combs based on optical nonlinearities, such as Kerr combs, any source based on nonlinear optics alone possesses fundamental bandwidth-density tradeoffs[3] due to the low parametric gain. This makes it unlikely that a dense nonlinearity-driven comb could ever be made as broadband as one based on a conventional solid-state laser (e.g., Ti:sapphire). However, the engineering of FM combs in broadband solid state gain media such as Ti:sapphire could potentially be an alternative strategy for the generation of ultrabroadband on-chip pulses, as the FM comb generation mechanism is not subject to the same efficiency limitations as passive modelocking, a central consideration in low-gain lasers.

ACKNOWLEDGMENTS

D.B. acknowledges the support from ONR (Grant No. N00014-21-1-2735), AFOSR (Grant No. FA9550-20-1-0192), and NSF (Grant No. ECCS-2046772); this research is funded in part by the Gordon and Betty Moore Foundation (Grant No. GBMF11446) to the University of Texas at Austin to support the work of D.B.

AUTHOR DECLARATIONS

Conflict of Interest

The authors have no conflicts to disclose.

Author Contributions

Mithun Roy and Tianyi Zeng contributed equally to this work.

Mithun Roy: Data curation (equal); Formal analysis (equal); Investigation (equal); Writing – original draft (lead); Writing – review & editing (equal). **Tianyi Zeng:** Data curation (equal); Formal analysis (equal); Investigation (equal); Writing – original draft (supporting); Writing – review & editing (equal). **David Burghoff:** Data curation (supporting); Funding acquisition (lead); Supervision (lead); Writing – review & editing (lead).

DATA AVAILABILITY

The data that support the findings of this study are available from the corresponding author upon reasonable request.

REFERENCES

[1]M.-G. Suh, Q.-F. Yang, K. Y. Yang, X. Yi, and K. J. Vahala, "Microresonator soliton dual-comb spectroscopy," Science **354**, 600–603 (2016).
[2]M. Yu, Y. Okawachi, A. G. Griffith, N. Picqué, M. Lipson, and A. L. Gaeta, "Silicon-chip-based mid-infrared dual-comb spectroscopy," Nat. Commun. **9**, 1869 (2018).
[3]D. T. Spencer, T. Drake, T. C. Briles, J. Stone, L. C. Sinclair, C. Fredrick, Q. Li, D. Westly, B. R. Ilic, A. Bluestone, N. Volet, T. Komljenovic, L. Chang, S. H. Lee, D. Y. Oh, M.-G. Suh, K. Y. Yang, M. H. P. Pfeiffer, T. J. Kippenberg, E. Norberg, L. Theogarajan, K. Vahala, N. R. Newbury, K. Srinivasan, J. E. Bowers, S. A. Diddams, and S. B. Papp, "An optical-frequency synthesizer using integrated photonics," Nature **557**, 81–85 (2018).
[4]P. Trocha, M. Karpov, D. Ganin, M. H. P. Pfeiffer, A. Kordts, S. Wolf, J. Krockenberger, P. Marin-Palomo, C. Weimann, S. Randel, W. Freude, T. J. Kippenberg, and C. Koos, "Ultrafast optical ranging using microresonator soliton frequency combs," Science **359**, 887–891 (2018).
[5]M.-G. Suh and K. J. Vahala, "Soliton microcomb range measurement," Science **359**, 884–887 (2018).
[6]V. Brasch, M. Geiselmann, T. Herr, G. Lihachev, M. H. P. Pfeiffer, M. L. Gorodetsky, and T. J. Kippenberg, "Photonic chip-based optical frequency comb using soliton Cherenkov radiation," Science **351**, 357–360 (2016).
[7]P. Del'Haye, A. Coillet, T. Fortier, K. Beha, D. C. Cole, K. Y. Yang, H. Lee, K. J. Vahala, S. B. Papp, and S. A. Diddams, "Phase-coherent microwave-to-optical link with a self-referenced microcomb," Nat. Photonics **10**, 516–520 (2016).
[8]C. Reimer, M. Kues, P. Roztocki, B. Wetzel, F. Grazioso, B. E. Little, S. T. Chu, T. Johnston, Y. Bromberg, L. Caspani, D. J. Moss, and R. Morandotti, "Generation of multiphoton entangled quantum states by means of integrated frequency combs," Science **351**, 1176–1180 (2016).
[9]Z. Yang, M. Jahanbozorgi, D. Jeong, S. Sun, O. Pfister, H. Lee, and X. Yi, "A squeezed quantum microcomb on a chip," Nat. Commun. **12**, 4781 (2021).
[10]T. Udem, J. Reichert, R. Holzwarth, and T. Hänsch, "Absolute optical frequency measurement of the cesium D_1 line with a mode-locked laser," Phys. Rev. Lett. **82**, 3568 (1999a).
[11]T. Udem, J. Reichert, R. Holzwarth, and T. W. Hänsch, "Accurate measurement of large optical frequency differences with a mode-locked laser," Opt. Lett. **24**, 881–883 (1999b).
[12]M. Singleton, P. Jouy, M. Beck, and J. Faist, "Evidence of linear chirp in mid-infrared quantum cascade lasers," Optica **5**, 948 (2018).
[13]J. Hillbrand, D. Auth, M. Piccardo, N. Opačak, E. Gornik, G. Strasser, F. Capasso, S. Breuer, and B. Schwarz, "In-phase and anti-phase synchronization in a laser frequency comb," Phys. Rev. Lett. **124**, 023901 (2020).
[14]B. Schwarz, J. Hillbrand, M. Beiser, A. M. Andrews, G. Strasser, H. Detz, A. Schade, R. Weih, and S. Höfling, "Monolithic frequency comb platform based on interband cascade lasers and detectors," Optica **6**, 890–895 (2019).
[15]L. A. Sterczewski, C. Frez, S. Forouhar, D. Burghoff, and M. Bagheri, "Frequency-modulated diode laser frequency combs at 2 Um wavelength," APL Photonics **5**, 076111 (2020).
[16]H. S. Stokowski, D. J. Dean, A. Y. Hwang, T. Park, O. T. Celik, T. P. McKenna, M. Jankowski, C. Langrock, V. Ansari, M. M. Fejer *et al.*, "Integrated frequency-modulated optical parametric oscillator," Nature **627**, 95–100 (2024).
[17]G. Villares, A. Hugi, S. Blaser, and J. Faist, "Dual-comb spectroscopy based on quantum-cascade-laser frequency combs," Nat. Commun. **5**, 5192 (2014).
[18]S. E. Harris and R. Targ, "FM oscillation of the He-Ne laser," Appl. Phys. Lett. **5**, 202–204 (1964).
[19]T. Maiman, "Stimulated optical radiation in ruby," Nature **187**, 493–494 (1960).
[20]S. Harris and O. McDuff, "Theory of FM laser oscillation," IEEE J. Quantum Electron. **1**, 245–262 (1965).
[21]A. Hugi, G. Villares, S. Blaser, H. C. Liu, and J. Faist, "Mid-infrared frequency comb based on a quantum cascade laser," Nature **492**, 229–233 (2012).
[22]D. Burghoff, T.-Y. Kao, N. Han, C. W. I. Chan, X. Cai, Y. Yang, D. J. Hayton, J.-R. Gao, J. L. Reno, and Q. Hu, "Terahertz laser frequency combs," Nat. Photonics **8**, 462–467 (2014).
[23]D. Burghoff, Y. Yang, D. J. Hayton, J.-R. Gao, J. L. Reno, and Q. Hu, "Evaluating the coherence and time-domain profile of quantum cascade laser frequency combs," Opt. Express **23**, 1190 (2015).
[24]A. Gordon, C. Y. Wang, L. Diehl, F. X. Kärtner, A. Belyanin, D. Bour, S. Corzine, G. Höfler, H. C. Liu, H. Schneider, T. Maier, M. Troccoli, J. Faist, and F. Capasso, "Multimode regimes in quantum cascade lasers: From coherent instabilities to spatial hole burning," Phys. Rev. A **77**, 053804 (2008).
[25]Y. Wang and A. Belyanin, "Active mode-locking of mid-infrared quantum cascade lasers with short gain recovery time," Opt. Express **23**, 4173–4185 (2015).
[26]C. Silvestri, L. L. Columbo, M. Brambilla, and M. Gioannini, "Coherent multi-mode dynamics in a quantum cascade laser: amplitude- and frequency-modulated optical frequency combs," Opt. Express **28**, 23846–23861 (2020).
[27]P. Tzenov, D. Burghoff, Q. Hu, and C. Jirauschek, "Analysis of operating regimes of terahertz quantum cascade laser frequency combs," IEEE Trans. Terahertz. Sci. Technol. **7**, 351–359 (2017).
[28]J. B. Khurgin, Y. Dikmelik, A. Hugi, and J. Faist, "Coherent frequency combs produced by self frequency modulation in quantum cascade lasers," Appl. Phys. Lett. **104**, 081118 (2014).
[29]G. Villares and J. Faist, "Quantum cascade laser combs: Effects of modulation and dispersion," Opt. Express **23**, 1651–1669 (2015).
[30]D. C. Cole, A. Gatti, S. B. Papp, F. Prati, and L. Lugiato, "Theory of Kerr frequency combs in Fabry-Perot resonators," Phys. Rev. A **98**, 013831 (2018).
[31]L. A. Lugiato, F. Prati, M. L. Gorodetsky, and T. J. Kippenberg, "From the Lugiato–Lefever equation to microresonator-based soliton Kerr frequency combs," Philos. Trans. R Soc., A **376**, 20180113 (2018).
[32]D. Burghoff, "Unraveling the origin of frequency modulated combs using active cavity mean-field theory," Optica **7**, 1781–1787 (2020).
[33]K. Y. Lau, I. Ury, and A. Yariv, "Passive and active mode locking of a semiconductor laser without an external cavity," Appl. Phys. Lett. **46**, 1117–1119 (1985).
[34]K. Sato, "100 GHz optical pulse generation using Fabry-Perot laser under continuous wave operation," Electron. Lett. **37**, 763–764 (2001).
[35]K. Sato, "Optical pulse generation using Fabry-Perot lasers under continuous-wave operation," IEEE J. Sel. Top. Quantum Electron. **9**, 1288–1293 (2003).
[36]R. Huber, M. Wojtkowski, and J. G. Fujimoto, "Fourier domain mode locking (FDML): A new laser operating regime and applications for optical coherence tomography," Opt. Express **14**, 3225–3237 (2006).
[37]M. Roy, Z. Xiao, S. Addamane, and D. Burghoff, "Fundamental scaling limits and bandwidth shaping of frequency-modulated combs," arXiv:2310.00028 (2024).
[38]H. Wang, J. Zhang, F. Cheng, N. Zhuo, S. Zhai, J. Liu, L. Wang, S. Liu, F. Liu, and Z. Wang, "Watt-level, high wall plug efficiency, continuous-wave room temperature quantum cascade laser emitting at 7.7 μm," Opt. Express **28**, 40155–40163 (2020).
[39]A. Khalatpour, A. K. Paulsen, C. Deimert, Z. R. Wasilewski, and Q. Hu, "High-power portable terahertz laser systems," Nat. Photonics **15**, 16–20 (2021).
[40]D. Burghoff, Y. Yang, and Q. Hu, "Computational multiheterodyne spectroscopy," Sci. Adv. **2**, e1601227 (2016).
[41]D. J. Benirschke, N. Han, and D. Burghoff, "Frequency comb ptychoscopy," Nat. Commun. **12**, 4244 (2021).
[42]G. Villares, S. Riedi, J. Wolf, D. Kazakov, M. J. Süess, P. Jouy, M. Beck, and J. Faist, "Dispersion engineering of quantum cascade laser frequency combs," Optica **3**, 252–258 (2016).

[43]F. Cappelli, L. Consolino, G. Campo, I. Galli, D. Mazzotti, A. Campa, M. S. de Cumis, P. C. Pastor, R. Eramo, M. Rösch, M. Beck, G. Scalari, J. Faist, P. D. Natale, and S. Bartalini, "Retrieval of phase relation and emission profile of quantum cascade laser frequency combs," Nat. Photonics **13**, 562–568 (2019).
[44]U. Senica, A. Dikopoltsev, A. Forrer, S. Cibella, G. Torrioli, M. Beck, J. Faist, and G. Scalari, "Frequency-modulated combs via field-enhancing tapered waveguides," Laser Photonics Rev. **17**, 2300472 (2023).
[45]I. Heckelmann, M. Bertrand, A. Dikopoltsev, M. Beck, G. Scalari, and J. Faist, "Quantum walk comb in a fast gain laser," Science **382**, 434–438 (2023).
[46]P. Täschler, M. Bertrand, B. Schneider, M. Singleton, P. Jouy, F. Kapsalidis, M. Beck, and J. Faist, "Femtosecond pulses from a mid-infrared quantum cascade laser," Nat. Photonics **15**, 919–924 (2021).
[47]P. Täschler, A. Forrer, M. Bertrand, F. Kapsalidis, M. Beck, and J. Faist, "Asynchronous upconversion sampling of frequency modulated combs," Laser Photonics Rev. **17**, 2200590 (2023).
[48]M. W. Day, M. Dong, B. C. Smith, R. C. Owen, G. C. Kerber, T. Ma, H. G. Winful, and S. T. Cundiff, "Simple single-section diode frequency combs," APL Photonics **5**, 121303 (2020).
[49]E. U. Rafailov, M. A. Cataluna, and W. Sibbett, "Mode-locked quantum-dot lasers," Nat. Photonics **1**, 395–401 (2007).
[50]H. Liu, D. Childs, T. Badcock, K. Groom, I. Sellers, M. Hopkinson, R. Hogg, D. Robbins, D. Mowbray, and M. Skolnick, "High-performance three-layer 1.3-μm InAs-GaAs quantum-dot lasers with very low continuous-wave room-temperature threshold currents," IEEE Photonics Technol. Lett. **17**, 1139–1141 (2005).
[51]M. J. R. Heck, A. Renault, E. A. J. M. Bente, Y. Oei, M. K. Smit, K. S. E. Eikema, W. Ubachs, S. Anantathanasarn, and R. NÖtzel, "Passively mode-locked 4.6 and 10.5 GHz quantum dot laser diodes around 1.55 mm with large operating regime," IEEE J. Select. Top. Quantum Electron. **15**, 634–643 (2009).
[52]R. Rosales, S. G. Murdoch, R. T. Watts, K. Merghem, A. Martinez, F. Lelarge, A. Accard, L. P. Barry, and A. Ramdane, "High performance mode locking characteristics of single section quantum dash lasers," Opt. Express **20**, 8649–8657 (2012).
[53]N. Opačak and B. Schwarz, "Theory of frequency-modulated combs in lasers with spatial hole burning, dispersion, and Kerr nonlinearity," Phys. Rev. Lett. **123**, 243902 (2019).
[54]C. Silvestri, M. Brambilla, P. Bardella, and L. L. Columbo, "Unified theory for frequency combs in ring and Fabry-Perot quantum cascade lasers: An order-parameter equation approach," arXiv:2403.06486 (2024).
[55]L. Humbard and D. Burghoff, "Analytical theory of frequency-modulated combs: Generalized mean-field theory, complex cavities, and harmonic states," Opt. Express **30**, 5376–5401 (2022).
[56]M. Piccardo, B. Schwarz, D. Kazakov, M. Beiser, N. Opačak, Y. Wang, S. Jha, J. Hillbrand, M. Tamagnone, W. T. Chen, A. Y. Zhu, L. L. Columbo, A. Belyanin, and F. Capasso, "Frequency combs induced by phase turbulence," Nature **582**, 360–364 (2020).
[57]B. Meng, M. Singleton, J. Hillbrand, M. Franckié, M. Beck, and J. Faist, "Dissipative Kerr solitons in semiconductor ring lasers," Nat. Photonics **16**, 142–147 (2022).
[58]H. Haus, "A theory of forced mode locking," IEEE J. Quantum Electron. **11**, 323–330 (1975a).
[59]H. A. Haus, "Theory of mode locking with a fast saturable absorber," J. Appl. Phys. **46**, 3049–3058 (1975b).
[60]N. Picqué and T. W. Hänsch, "Frequency comb spectroscopy," Nat. Photonics **13**, 146–157 (2019).
[61]S. Barbieri, M. Ravaro, P. Gellie, G. Santarelli, C. Manquest, C. Sirtori, S. P. Khanna, E. H. Linfield, and A. G. Davies, "Coherent sampling of active mode-locked terahertz quantum cascade lasers and frequency synthesis," Nat. Photonics **5**, 306–313 (2011).
[62]F. Keilmann, C. Gohle, and R. Holzwarth, "Time-domain mid-infrared frequency-comb spectrometer," Opt. Lett. **29**, 1542 (2004).
[63]I. Coddington, N. Newbury, and W. Swann, "Dual-comb spectroscopy," Optica **3**, 414 (2016).
[64]B. Dong, M. Dumont, O. Terra, H. Wang, A. Netherton, and J. E. Bowers, "Broadband quantum-dot frequency-modulated comb laser," Light. Sci. Appl. **12**, 182 (2023).